Available online at www.sciencedirect.com
SCIENCE DIRECT®
Microporous and Mesoporous Materials 90 (2006) 5–15
MICROPOROUS AND MESOPOROUS MATERIALS
www.elsevier.com/locate/micromeso

Synthesis and structure of Mu-33, a new layered aluminophosphate $|((CH_3)_3CNH_3^+)_{16}(H_2O)_4|[Al_{16}P_{24}O_{88}(OH)_8]$

Claire Marichal [a,*], Jean Michel Chézeau [a], Mélanie Roux [a], Joël Patarin [a], José Luis Jordá [b,1], Lynne B. McCusker [b,*], Christian Baerlocher [b], Philip Pattison [c,d]

[a] *Laboratoire de Matériaux à Porosité Contrôlée, ENSCMu, Université de Haute Alsace, CNRS-UMR 7016, 3 rue Alfred Werner, F-68093 Mulhouse Cedex, France*
[b] *Laboratorium für Kristallographie, ETH Hönggerberg, CH-8093 Zürich, Switzerland*
[c] *Swiss-Norwegian Beamline, ESRF, BP220, F-38043 Grenoble Cedex, France*
[d] *Laboratoire de Cristallographie, EPFL, CH-1015 Lausanne, Switzerland*

Received 11 April 2005; received in revised form 8 June 2005; accepted 10 June 2005
Available online 28 July 2005

Dedicated to the late Denise Barthomeuf, George Kokotailo and Sergey P. Zhdanov in appreciation of their outstanding contributions to zeolite science

Abstract

Mu-33, a new layered aluminophosphate with an Al/P ratio of 0.66, was obtained from a quasi non-aqueous synthesis in which *tert*-butylformamide (*t*BF) was the main solvent and only limited amounts of water were present. During the synthesis, *t*BF decomposed and the resulting protonated *tert*-butylamine is occluded in the as-synthesized material. The approximate structure was determined from data collected on a microcrystal ($200 \times 25 \times 5\ \mu m^3$) at the European Synchrotron Radiation Facility (ESRF) in Grenoble, but the quality of these data did not allow satisfactory refinement. Therefore the structure was refined using high-resolution powder diffraction data, also collected at the ESRF. The structure ($P2_1/c$, $a = 9.8922(6)$ Å, $b = 26.180(2)$ Å, $c = 16.729(1)$ Å and $\beta = 90.4(1)°$) consists of anionic aluminophosphate layers that can be described as a six-ring honeycomb of alternating corner-sharing AlO_4 and PO_4 tetrahedra with additional P-atoms above and below the honeycomb layer bridging between Al-atoms. The *tert*-butylammonium ions and water molecules located in the interlayer spacing interact via hydrogen-bonds with the terminal oxygens of the P-atoms. The characterization of this new aluminophosphate by ^{13}C, ^{31}P, ^{1}H–^{31}P heteronuclear correlation (HETCOR) and ^{27}Al 3QMAS solid state NMR spectroscopy is also reported.

Keywords: ^{27}Al and ^{31}P solid state NMR; Microcrystal; Rietveld refinement; Layered aluminophosphate

1. Introduction

Since the seminal paper by Wilson et al. on the synthesis of aluminophosphate molecular sieves in 1982 [1], a large variety of these materials have been prepared. They are usually characterized by an Al/P ratio of one and a neutral three-dimensional aluminophosphate framework of alternating, corner-sharing AlO_4 and PO_4 tetrahedra. Some members of this $AlPO_4$-family of microporous materials have structures analogous to

* Corresponding authors. Tel.: +33 3 89 33 67 31; fax: +33 3 89 33 68 85 (C. Marichal), fax: +41 1 632 1133 (L.B. McCusker).
E-mail addresses: c.marichal@univ-mulhouse.fr (C. Marichal), lynne.mccusker@mat.ethz.ch (L.B. McCusker).
[1] Present address: Instituto de Tecnología Química, Universidad Politécnica de Valencia, E-46022 Valencia, Spain.

1387-1811/$ - see front matter © 2005 Elsevier Inc. All rights reserved.
doi:10.1016/j.micromeso.2005.06.008

those of zeolites. For example, $AlPO_4$-**GIS** and $AlPO_4$-20 are isostructural with gismondine (Framework type: **GIS**) and sodalite (Framework type: **SOD**), respectively. However, other compounds, such as $AlPO_4$-11 (Framework type: **AEL**) and VPI-5 (Framework type: **VFI**) do not have zeolite counterparts.

The synthesis of these solids is usually performed in aqueous medium, but a number of new phosphate-based materials have been prepared from non-aqueous or quasi non-aqueous media. As a result of such syntheses, using an organic solvent and only restricted amounts of water, numerous layered aluminophosphates have been obtained [2–9]. Under these conditions, hydrolysis and condensation reaction kinetics are slower than those of comparable hydrothermal systems. Several compositions of layered structures have been reported (e.g. $[Al_3P_4O_{16}]^{3-}$, $[Al_2P_3O_{12}H_x]^{(3-x)-}$ $(1 \leqslant x \leqslant 2)$ [10], $[AlP_2O_8]^{3-}$ [11,12], $[Al(HPO_4)_2(H_2O)_2]^-$[13] or $[Al_4P_5O_{20}H]^{2-}$ [9]), and most are characterized by an Al/P ratio of less than one. These compounds contain layers consisting of 4.6^2, 4.6.8 and 4.6.12 nets.

The alkylformamide family of solvents was used in a series of quasi non-aqueous syntheses to produce a monoclinic variant of $|AlPO_4|$-**SOD** [14], the two layered aluminophosphates, Mu-4 [9] and Mu-7 [15], and, more recently, the two new gallophosphates Mu-30 [16] and Ea-TREN-GaPO [17]. In all cases, with the exception of $|AlPO_4|$-**SOD**, the organic solvent partly decomposed into the corresponding amine, which was occluded in the final structure.

The title compound Mu-33 (Mu for Mulhouse) was prepared in a quasi non-aqueous synthesis procedure using *tert*-butylformamide (*t*BF) as the main solvent. Details of its synthesis, of its characterization by ^{13}C, ^{27}Al, ^{31}P, ^1H–^{31}P heteronuclear correlation (HETCOR) and ^{27}Al 3QMAS solid state NMR spectroscopy, and of its structure analysis are given in the following sections.

2. Experimental section

2.1. Sample preparation

Mu-33 was first prepared from a gel containing mainly *tert*-butylformamide (*t*BF) as the solvent [18]. In order to obtain a pure material, several experiments were performed and the amounts of the reactants were optimized. Typically, 1.23 g of pseudo-boemite (Condéa hydrated alumina, water loss at 600 °C: 22.2 wt%) was slowly added to 3.30 g of 85% orthophosphoric acid (Fluka). The resulting gel was stirred until it was homogeneous. Finally, 8.0 g of an aqueous *tert*-butylformamide solution (BDH, analytical grade) was added to the mixture. The gel, with the composition 0.66 Al_2O_3: 1.0 P_2O_5: 3.0 H_2O: 5.9 *t*BF, was heated in a Teflon-lined stainless-steel autoclave at 170 °C under autogeneous pressure for seven days. The solid recovered by filtration was washed with distilled water and dried at 60 °C overnight.

2.2. Characterization

The as-synthesized product was characterized initially by X-ray powder diffraction using a STOE STADI-P diffractometer equipped with a curved germanium 111 primary monochromator and a linear position-sensitive detector ($CuK\alpha_1$ radiation, $\lambda = 1.5406$ Å).

The morphology and average size of the crystals were determined by scanning electron microscopy (SEM) using a Philips XL30 microscope.

Thermogravimetric (TGA) and differential thermal (DTA) analyses to determine the amount of organic species and water occluded in the as-made solid were performed on a Setaram Labsys thermoanalyser by heating the as-synthesized material under air at a rate of 5 °C min^{-1} up to 750 °C.

C and N analyses were performed by coulometric and catharometric measurements, respectively. The Al and P content were determined by inductively coupled plasma emission spectroscopy.

^{31}P, ^{27}Al, ^{13}C and ^1H NMR measurements were carried out at room temperature using a Bruker DSX 400 spectrometer ($B_0 = 9.4$T), at frequencies of 161.9, 104.2, 100.2 and 400.1 MHz, respectively. ^{31}P Magic Angle Spinning (MAS) NMR experiments were performed using standard double bearing probes with either 4 or 2.5 mm diameter ZrO_2 rotors, and data were acquired using spinning frequencies between 3.5 and 25 kHz, a $\pi/2$ pulse duration of 3.5 μs and a recycle delay of 200 s. ^1H–^{31}P Cross-Polarization Magic Angle Spinning (CPMAS) spectra were recorded using conventional Hartmann–Hahn matching with a spinning frequency of 4 and 25 kHz, a ^1H $\pi/2$ pulse duration of 4 μs, contact times ranging from 500 μs to 2 ms, and a recycle delay of 4 s. ^1H–^{31}P heteronuclear correlation (HETCOR) experiments were performed at a spinning frequency of 25 kHz, with a contact time of 500 μs. ^{27}Al MAS NMR spectra were recorded using a 2.5 mm Bruker MAS probe, a spinning frequency of 15 kHz and a recycle delay of 1 s. The experimental conditions for the ^{27}Al 3QMAS experiment are described elsewhere [19]. ^{13}C MAS NMR experiments were realized with high power ^1H decoupling, a $\pi/2$ pulse duration of 4.5 μs, and a recycle delay of 60 s. Chemical shifts were referenced to an external standard: 85% H_3PO_4 (^{31}P), an aqueous solution of $Al(NO_3)_3$(^{27}Al) and TMS (^1H and ^{13}C).

Although the crystals in the sample appeared to be quite large in two dimensions (see Fig. 1), they proved to be too thin for single-crystal data collection on a laboratory instrument. However, it was possible to collect data on one of these microcrystals using the Oxford Dif-

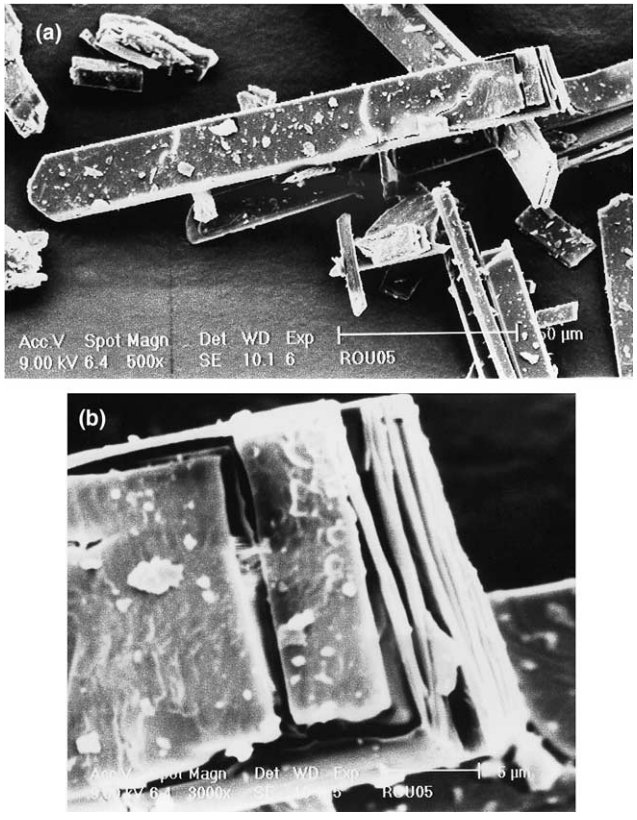

Fig. 1. SEM images of the lamellar aluminophosphate Mu-33.

Table 1
X-ray data collection parameters for Mu-33

Microcrystal		
Size		$200 \times 25 \times 5$ µm
Synchrotron facility		SNBL at ESRF
Beamline		BM01A
Wavelength		0.7500 Å
Instrument		Oxford Diffraction KM6
Detector		Onyx CCD
Image size		$1K \times 1K$
Temperature		120 K
Beam size		0.5×0.5 mm
Sample-detector distance		80 mm
Exposure time per frame		5 s
Omega rotation per frame		1°
Reflections		
Measured		91,205
Unique		9903
R_{int}		0.0583
Powder		
Synchrotron facility		SNBL at ESRF
Beamline		BM01B
Wavelength		0.79999 Å
Diffraction geometry		Debye–Scherrer
Analyzer crystal		Si 111
Sample		Rotating 1.0 mm capillary
2θ range		1.0–43°2θ
Step size		0.002°2θ
Time per step	1.0–15.5°2θ	1.0 s
	15.5–20.5°2θ	2.0 s
	20.5–43.0°2θ	4.0 s

fraction KM6 kappa diffractometer equipped with an Onyx CCD area detector on station BM01A of the Swiss-Norwegian Beamlines (SNBL) at the European Synchrotron Radiation Facility (ESRF) in Grenoble. For data collection, a microcrystal (ca $200 \times 25 \times 5$ µm^3) was mounted on a glass fiber using Fomblin oil and inserted directly into the cold stream of an Oxford Cryostream N_2 gas cooler operating at 120 K. These data were of sufficient quality to allow the structure to be solved, but structure refinement proved to be difficult. Therefore, high-resolution powder diffraction data were collected using the powder diffractometer on station BM01B of the SNBL, in the hope that these would be more suitable for refinement. Details of both data collections are given in Table 1.

3. Results

3.1. Characterization

The morphology of the Mu-33 crystals is shown in Fig. 1(a). Acicular crystals of various sizes were observed, and the closeup view given in Fig. 1(b) shows that the needles are in fact stacks of plate-like crystallites. This is indicative of a lamellar material.

The C, N, P and Al content was determined by chemical bulk analysis to be 19.63, 5.38, 18.00 and 10.70 wt%, respectively. The Al/P molar ratio is close to 0.66, which is similar to that observed for several other lamellar aluminophosphates [2,10]. However, the experimental C/N molar ratio of 4 was different from the value expected for *tert*-butylformamide (5C:1N), suggesting that the solvent might have decomposed into carbon monoxide and *tert*-butylamine (*t*BA) during synthesis. This was later confirmed by ^{13}C NMR spectroscopy (see below). As previously shown for other phosphate-based materials synthesized in the presence of alkylformamide [9,15,16], the in situ release of the corresponding protonated amine during the synthesis appears to be a key step in the crystallization of this lamellar aluminophosphate. Indeed, experiments using *tert*-butylamine in the starting mixture directly did not lead to the crystallization of this material.

The thermal behavior of Mu-33 was investigated by TG/DTA thermal analysis (Fig. 2). The total weight loss occurs in two steps. The first, below 200 °C (2.5 wt%), corresponds to the loss water. It leads to a weak and broad endothermic peak on the DTA curve. The second, between 200 and 800 °C (30.5 wt%), is associated with at least two endothermic components on the DTA curve. This probably corresponds to desorption and decomposition of the organic template, to the removal of water arising from dehydroxylation reactions (presence of P–OH groups) and to the collapse of the aluminophosphate framework. The exothermic signal, which is

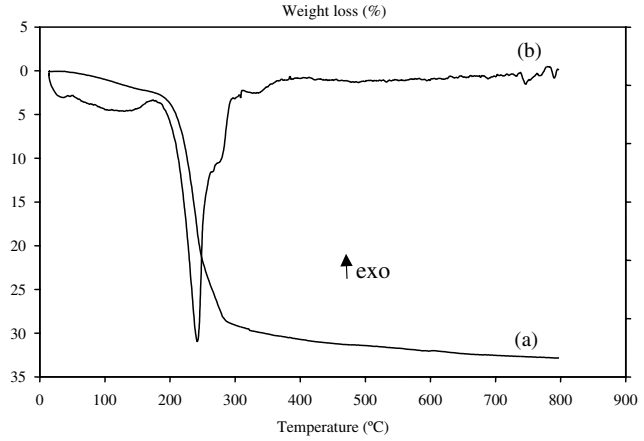

Fig. 2. Thermal analysis of the aluminophosphate Mu-33 in air. (a) TGA and (b) DTA.

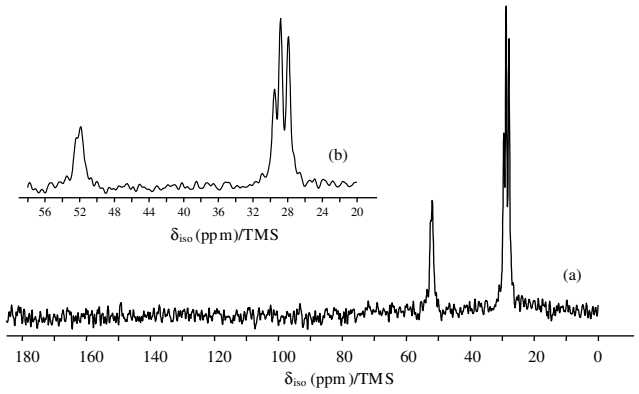

Fig. 3. ^{13}C MAS NMR with ^{1}H decoupling of the as-synthesized Mu-33 at $\nu_r = 4$ kHz. (a) Full spectrum and (b) spectral region between 58 and 20 ppm.

expected from the oxidation of the *t*BA, is probably masked by the overhelming endothermic collapse of the structure. XRD analysis of the residue left after heating to 800 °C shows that the material had transformed into a dense $AlPO_4$-tridymite phase.

According to the thermal and chemical analyses and the structure determination, the following chemical formula has been proposed for the as-synthesized Mu-33 sample: $4[((CH_3)_3CNH_3^+)_4[Al_4P_6O_{22}(OH)_2](H_2O)]$.

The amine molecules were considered as protonated in order to compensate the negative charge of the inorganic layer. This was confirmed by ^{13}C NMR spectroscopy (see below).

3.2. Solid state NMR study

3.2.1. ^{13}C MAS NMR

The ^{1}H decoupled ^{13}C MAS NMR spectrum of Mu-33 (Fig. 3) exhibits one resonance at 52 ppm (quaternary carbon of the *tert*-butyl groups) and three more at 29.5, 28.9 and 28 ppm (the three methyl groups of *t*BA). The presence of three resolved resonances for the methyl groups indicates that there are at least three non-equivalent methyl positions in the structure. Note that although a quantitative ^{13}C MAS NMR experiment rather than a ^{1}H–^{13}C CPMAS experiment was performed, no signal near 160 ppm that could correspond to the carbonyl groups of the *tert*-butylformamide is observed in Fig. 3. This result, in agreement with chemical analysis data, indicates that *tert*-butylamine (*t*BA) and not *tert*-butylformamide is occluded in the structure. The ^{13}C isotropic chemical shifts for protonated and non-protonated *t*BA in the liquid state are at 27.7 and 32.9 ppm, respectively for the methyl groups, and at

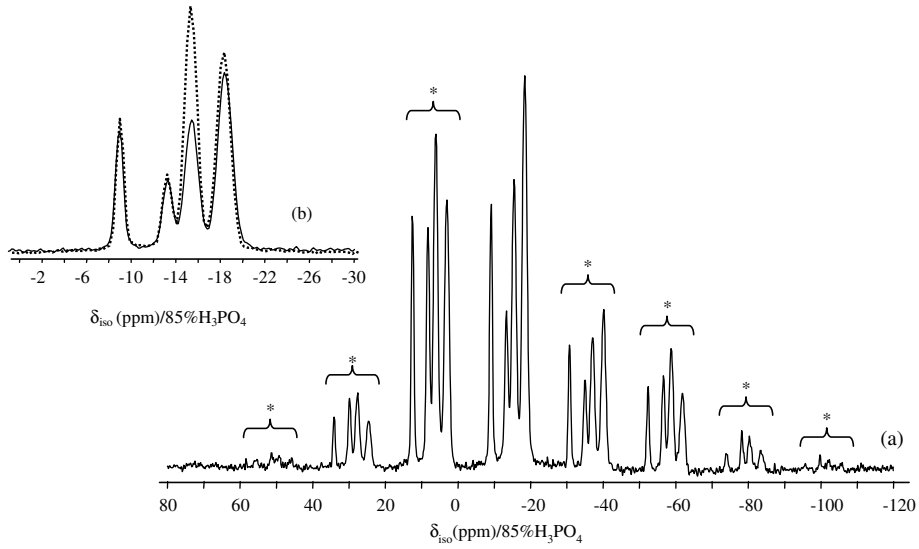

Fig. 4. ^{31}P MAS NMR spectra of the as-synthesized Mu-33 at $\nu_r = 4$ kHz. (a) Full spectrum, (b) MAS (line) and ^{1}H/^{31}P CPMAS $\tau = 500$ μs (dotted line) in the spectral region between 0 and −30 ppm. Spinning side bands are indicated by (*).

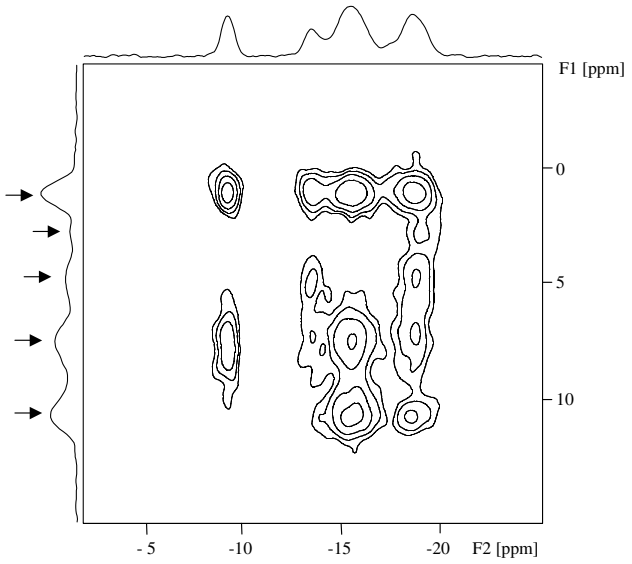

Fig. 5. ^{1}H–^{31}P HETCOR NMR experiment performed on the as-synthesized Mu-33 together with F1 (^{1}H MAS NMR spectrum) and F2 (^{31}P MAS NMR spectrum) projections. Arrows indicate the ^{1}H NMR components.

52.5 and 47.2 ppm, respectively for the quaternary carbon. Thus, as suggested in the previous section, the *t*BA occluded in Mu-33 appears to be protonated.

3.2.2. ^{31}P MAS NMR

Four resonances are observed in the ^{31}P MAS NMR spectrum of Mu-33 at −18.4, −15.5, −13.4 and −9.2 ppm with the relative intensities 2:2:1:1, respectively (Fig. 4). This indicates the presence of at least four (six if all have the same multiplicity) non-equivalent crystallographic sites for P. Chemical shift anisotropies of the P resonances range from −52 to −73 ppm with asymmetry parameters between 0.25 and 0.55 (simulations not reported). ^{1}H–^{31}P cross-polarization experiments, with a short (500 μs) contact time in order to avoid spin diffusion (Fig. 4(b)), significantly enhance the resonance at −15.5 ppm and to a lesser extent the one at −18.4 ppm, indicating a close proximity of these P-sites to protons from the template and/or water molecules.

In order to get some insight into the H–P connectivities in Mu-33, a ^{1}H–^{31}P heteronuclear correlation experiment was performed (Fig. 5). The F1 projection in Fig. 5 corresponds to the ^{1}H MAS NMR spectrum and exhibits five resonances at 1.1, 3.1, 5.1, 7.7 and 11.1 ppm (see arrows). According to liquid state NMR data, the resonances at 1.1 and 7.7 can be assigned to the methyl and the amine groups of *t*BA, respectively. The resonances at 5.1 and 11.1 ppm might correspond to "free" water and "hydrogen-bonded" water, respectively. No "free" water was detected by TG, but this may be a result of the fact that the state of hydration was not controlled in those experiments. Finally, the resonance at 3.1 ppm might be assigned to P–OH groups. All ^{31}P resonances are correlated with the ^{1}H resonance at 1.1 ppm, which indicates that the methyl groups of the template molecules are in close proximity to the framework. Similarly, the protons from the amine

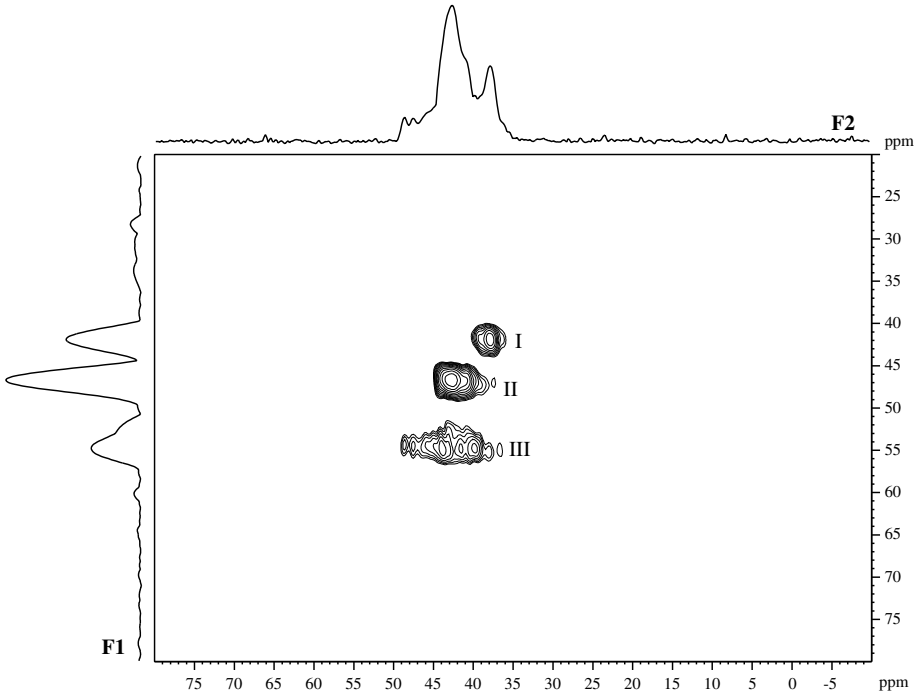

Fig. 6. ^{27}Al 3Q MAS NMR spectrum of the as-synthesized Mu-33 together with F1 and F2 projections.

(7.7 ppm) are also correlated with all P resonances. Note that the ^{1}H resonance at 3.1 ppm is correlated only with the ^{31}P resonance at −18.4 ppm, so these P-atoms can be assumed to have a terminal hydroxyl group. H-bonded water (11.1 ppm resonance) is in close proximity to the P-atoms associated with the ^{31}P resonances at −18.4 and −15.5 ppm.

3.2.3. ^{27}Al MAS NMR

The ^{27}Al MAS NMR spectrum of Mu-33 (Fig. 6, see F2 projection) shows a broad resonance between 35 and 50 ppm, indicating that the framework contains neither five-nor six-coordinated aluminum, which would show resonances around 10 and 0 ppm, respectively [20]. In order to remove second order quadrupolar broadening and to elucidate the number of distinct crystallographic aluminum sites, a triple quantum MAS NMR (3QMAS) experiment was performed (Fig. 6). The F1 projection indicates the presence of at least three distinct tetrahedral aluminum sites. According to the shape of the correlations, sites I to III possess increasing quadrupolar coupling constants. Indeed, the spreading (along the F2 dimension) of the correlation increases from correlation I to III indicating that the site corresponding to correlation III is more distorted than the others. Unfortunately, precise values for these quadrupolar coupling constants could not be determined, because of the lack of singularities on the respective quadrupolar lineshapes.

3.3. Structure solution and refinement

The X-ray diffraction data collected on the microcrystal of Mu-33 were indexed ($P2_1/c$, $a = 9.886$ Å, $b = 25.914$ Å, $c = 16.770$ Å, $\beta = 90.29°$) and the spots integrated using the Crysalis RED software package [21]. These data were then used as input to the direct methods program SHELXL-97 [22]. The complete structure, consisting of an aluminophosphate layer, four independent *t*BA species and one water molecule, was found. Unfortunately, the data proved to be of insufficient quality for refinement, so the structure analysis

Table 2
Crystallographic data from the Rietveld refinement of Mu-33

Chemical composition	$\|((CH_3)_3CNH_3^+)_{16}(H_2O)_4\|[Al_{16}P_{24}O_{92}(OH)_8]$				
Unit cell					
a					9.8922(6) Å
b					26.180(2) Å
c					16.729(1) Å
β					90.4(1)°
Space group					$P2_1/c$
Standard peak for peak shape function (*hkl*, 2*θ*)					
3.6–40°2*θ*					1 1 0, 4.96°
2.5–3.6°2*θ*					0 2 0, 3.50°
Peak range (number of FWHM)					20
Preferred orientation					
Vector					0 1 0
Factor					1.179(1)
Number of observations					18392
Number of contributing reflections					2836
Number of geometric restraints[a]					303
P–O	1.53(1) Å	24	C–H	0.950(1) Å	36
Al–O	1.73(1) Å	16	N–H	0.950(1) Å	12
O–P–O	109.5(1.0)°	36	O–H	0.950(1) Å	2
O–Al–O	109.5(1.0)°	24	H–N–C	109.5(1.0)°	12
P–O–Al	145(8)°	16	C–C–H	109.5(1.0)°	36
C–N	1.488(5) Å	4	H–N–H	109.5(1.0)°	12
C–C	1.534(5) Å	12	H–C–H	109.5(1.0)°	36
N–C–C	109.5(1.0)°	12	H–O–H	109.5(1.0)°	1
C–C–C	109.5(1.0)°	12			
Number of parameters					329
Structural (non-H)		170			
Structural (H)		150			
Profile		12			
R_F					0.032
R_{wp}					0.090
R_{exp}					0.050

[a] The numbers given in parentheses are the esd's assumed for each of the restraints. Each restraint was given a weight equivalent to the reciprocal of its esd.

Table 3
Positional, thermal and occupancy parameters for Mu-33[a]

Atom	x	y	z	U_{iso}(×100 Å^2)
P(1)	0.1038(4)	0.7388(2)	0.8343(2)	2.82(5)[b]
P(2)	0.9802(4)	0.6698(2)	0.6222(2)	2.82[b]
P(3)	0.5332(4)	0.6497(2)	0.8526(2)	2.82[b]
P(4)	0.6457(4)	0.7986(2)	0.8275(2)	2.82[b]
P(5)	0.9066(4)	0.8232(2)	0.5674(2)	2.82[b]
P(6)	0.4279(4)	0.7717(2)	0.5930(2)	2.82[b]
Al(1)	0.1387(4)	0.7451(2)	0.0238(2)	2.74(7)[c]
Al(2)	0.6625(4)	0.7715(2)	0.4766(2)	2.74[c]
Al(3)	0.8630(4)	0.7617(2)	0.7227(2)	2.74[c]
Al(4)	0.3984(4)	0.7471(2)	0.7736(2)	2.74[c]
O(1)	0.1134(7)	0.7578(3)	0.9206(4)	2.47(5)[d]
O(2)	0.4872(7)	0.7952(3)	0.8183(4)	2.47[d]
O(3)	0.4194(7)	0.7437(3)	0.6690(4)	2.47[d]
O(4)	0.8975(7)	0.6307(3)	0.5747(4)	2.47[d]
O(5)	0.2299(6)	0.7564(3)	0.7925(4)	2.47[d]
O(6)	0.5523(7)	0.7531(3)	0.5523(4)	2.47[d]
O(7)	0.0909(7)	0.6828(3)	0.8282(4)	2.47[d]
O(8)	0.8690(8)	0.8779(3)	0.5517(4)	2.47[d]
O(9)	0.9859(6)	0.7666(3)	0.7992(4)	2.47[d]
O(10)	0.3027(7)	0.7378(3)	0.0413(4)	2.47[d]
O(11)	0.6943(7)	0.8542(3)	0.8194(4)	2.47[d]
O(12)	0.4370(7)	0.8288(3)	0.6061(4)	2.47[d]
O(13)	0.6438(7)	0.6287(3)	0.7984(4)	2.47[d]
O(14)	0.8792(7)	0.8128(3)	0.6564(4)	2.47[d]
O(15)	0.4468(7)	0.6050(3)	0.8813(4)	2.47[d]
O(16)	0.8775(7)	0.7029(3)	0.6739(4)	2.47[d]
O(17)	0.8233(7)	0.7855(3)	0.5158(4)	2.47[d]
O(18)	0.0709(7)	0.7033(3)	0.5699(4)	2.47[d]
O(19)	0.6853(7)	0.7801(3)	0.9120(4)	2.47[d]
O(20)	0.4367(7)	0.6876(3)	0.8124(4)	2.47[d]
O(21)	0.6004(7)	0.6736(3)	0.9266(4)	2.47[d]
O(22)	0.0591(7)	0.8114(3)	0.5493(4)	2.47[d]
O(23)	0.7072(6)	0.7612(3)	0.7663(4)	2.47[d]
O(24)	0.0755(7)	0.6429(3)	0.6847(4)	2.47[d]
Ow	0.2761(9)	0.6180(5)	0.0102(5)	6.2[e]
N(1)	0.8832(9)	0.6115(4)	0.8790(5)	6.2(1)[e]
C(2)	0.920(1)	0.5566(4)	0.8661(5)	6.2[e]
C(3)	0.809(1)	0.5243(4)	0.9054(6)	6.2[e]
C(4)	0.928(1)	0.5480(5)	0.7746(5)	6.2[e]
C(5)	1.0587(9)	0.5488(4)	0.9063(5)	6.2[e]
N(6)	0.6425(9)	0.8939(4)	0.6640(5)	6.2[e]
C(7)	0.5754(9)	0.9438(4)	0.6793(6)	6.2[e]
C(8)	0.551(1)	0.9669(5)	0.5949(5)	6.2[e]
C(9)	0.4426(9)	0.9351(4)	0.7265(6)	6.2[e]
C(10)	0.6786(9)	0.9761(4)	0.7252(5)	6.2[e]
N(11)	−0.0613(8)	0.6418(3)	0.4084(5)	6.2[e]
C(12)	0.0350(9)	0.5988(4)	0.3863(5)	6.2[e]
C(13)	0.0563(9)	0.6055(4)	0.2960(5)	6.2[e]
C(14)	−0.0384(9)	0.5480(4)	0.4034(5)	6.2[e]
C(15)	0.1737(9)	0.6021(5)	0.4305(6)	6.2[e]
N(16)	0.6214(9)	0.6469(4)	0.6315(5)	6.2[e]
C(17)	0.5311(9)	0.6062(4)	0.5986(5)	6.2[e]
C(18)	0.599(1)	0.5540(4)	0.6163(6)	6.2[e]
C(19)	0.535(1)	0.6124(4)	0.5055(5)	6.2[e]
C(20)	0.3833(9)	0.6122(4)	0.6267(5)	6.2[e]

[a] Numbers in parentheses are the esd's in the units of the least significant digit given. Values without an esd were not refined. Calculated hydrogen positions not included.
[b–e] Thermal parameters with the same superscript were constrained to be equal.

was continued with high-resolution powder diffraction data.

Rietveld refinement was performed using the program XRS-82 [23] starting with the model obtained from SHELXL-97 and with geometric restraints on all interatomic distances and angles. Initially, these restraints were given high weight to guide the structure to a chemically sensible minimum, and then the weighting factor was reduced to 1. A mismatch between the observed and calculated patterns was traced to the presence of some preferred orientation in the sample along the [0 1 0] direction (perpendicular to the aluminophosphate layers). Once this factor had been included, refinement proceeded smoothly.

Positions for the H-atoms on the *t*BA and water molecules were calculated and added to the model with strong restraints to simulate "riding H-atoms". In view of the NMR results (previous section), the *t*BA species were assumed to be protonated. Two other protons (8 per unit cell) are assumed to be associated with the terminal oxygens at O(15) and O(24) of the POOH groups (phosphorus sites P3 and P2), but their exact location was not obvious, so they were not included in the final model. To keep the number of parameters to a minimum, displacement parameters for similar atoms were constrained to be equal. Refinement of all parameters eventually converged with $R_F = 0.032$, $R_{wp} = 0.090$ and $R_{exp} = 0.050$. The details of the refinement are given in Table 2, the final atomic parameters in Table 3 and selected distances and angles in Table 4. The fit of the

Table 4
Selected interatomic distances (Å) and angles (deg.) for Mu-33

P–O	Min	1.47	Al–O	Min	1.66
	Max	1.59		Max	1.77
	Avg	1.53		Avg	1.73
O–P–O	Min	104.8	O–Al–O	Min	103.9
	Max	114.8		Max	114.1
	Avg	109.5		Avg	109.4
Al–O–P	Min	126.4			
	Max	161.8			
	Avg	143.8			
C–N	Min	1.50	C–C	Min	1.53
	Max	1.52		Max	1.57
	Avg	1.49		Avg	1.55
N–C–C	Min	104.2	C–C–C	Min	105.5
	Max	113.3		Max	116.1
	Avg	107.6		Avg	111.2
N(1)–O(7)		2.90(6)	N(6)–O(8)		2.96(14)
N(1)–O(8)		2.90(2)	N(6)–O(11)		2.84(5)
N(1)–O(13)		2.75(12)	N(6)–O(12)		2.82(7)
N(11)–O(4)		2.83(4)	N(16)–O(4)		2.93(9)
N(11)–O(11)		2.83(13)	N(16)–O(13)		2.83(2)
Ow–O(12)		2.65(10)			
Ow–O(15)		2.77(13)			
Ow–O(22)		2.91(5)			

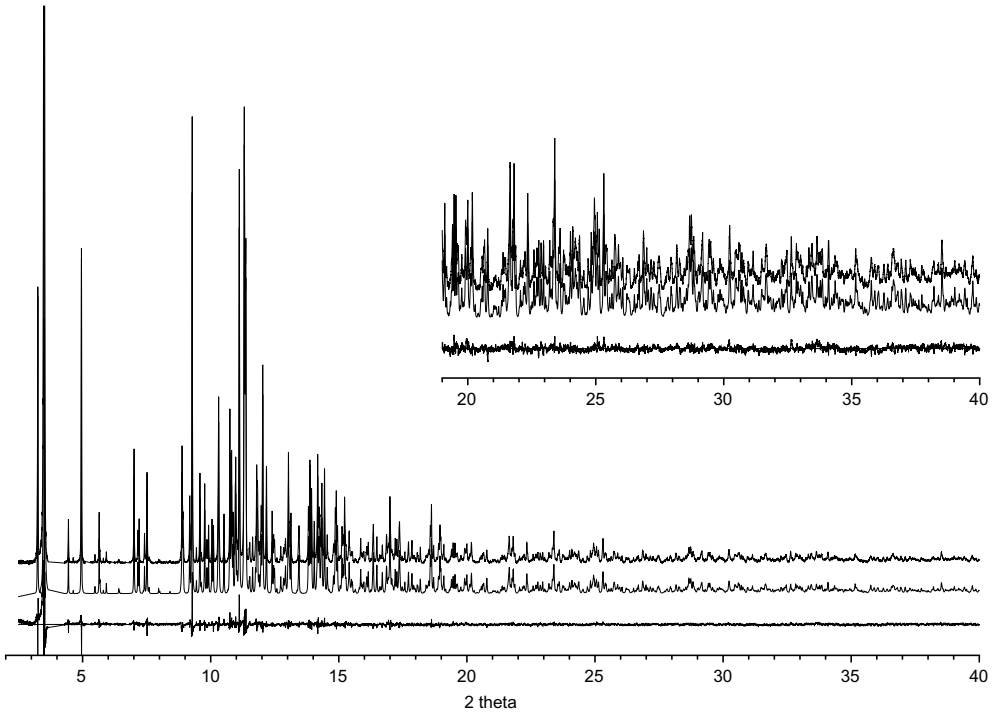

Fig. 7. The observed (top), calculated (middle) and difference (bottom) profiles for the Rietveld refinement of Mu-33. To show more detail, the first peak has been cut at 20% of its full intensity and the scale for the second half of the pattern has been increased by a factor of 5 in the inset.

profile calculated for this model to the experimental data is shown in Fig. 7. Neutral scattering factors were used for all atoms.

4. Discussion

The structure of Mu-33 can be described in terms of an aluminophosphate layer with *t*-butylammonium ions and water molecules hydrogen-bonded to the terminal oxygens on both sides of the layer. These gently corrugated sheets are stacked following the 2_1 axis along the [0 1 0] direction (Fig. 8(a)). The aluminophosphate layer itself can be viewed as a six-ring honeycomb of alternating tetrahedrally coordinated Al- and P-atoms in which additional P-atoms above and below the layer bridge between adjacent Al-atoms. Thus, each of the four crystallographically distinct Al-sites is connected to four P-atoms via oxygen bridges, while four of the crystallographically distinct P-sites are connected to three Al-atoms and the other two (P2 and P3) to two (Fig. 8(b)). The coordination spheres of the former are completed with single terminal oxygen species (P═O) and those of the latter with two (P═O and P–OH). These terminal oxygens serve as hydrogen-bond acceptors for the four crystallographically distinct *t*-butylammonium ions and the water molecule (Figs. 8(c) and 9).

Careful consideration of the structure combined with information from the 2D ^{1}H–^{31}P HETCOR experiment (Fig. 5) allows an assignment for all ^{31}P resonances to be proposed. Phosphorus sites P2 and P3 are both connected to two aluminums via oxygens and have one terminal oxygen (H-bonded to two amines) and one hydroxyl group. They have similar environments (see the scheme in Fig. 9), but P3 is also H-bonded to the water molecule via the hydroxyl group (O15). Therefore P2 and P3 are assigned to the ^{31}P resonance at −18.4 ppm, which exhibits correlations with the ^{1}H resonances at 3.1 ppm (P–OH) and 11.1 ppm (H-bonded water) in addition to the tBA^{+} resonances.

Both P5 and P6 are connected to three aluminums via oxygens and have one terminal oxygen (P═O). In the case of P5, this oxygen is H-bonded to two amines, whereas for P6 it is H-bonded to one amine and one water molecule. The oxygen at O22, bridging from P5 to Al1 is also H-bonded to the water molecule (see Fig. 9). As these two phosphorus sites are similar, they are assigned to the ^{31}P resonance at −15.5 ppm, which is correlated with the ^{1}H resonance at 11.1 ppm (H-bonded water). The correlation between the ^{31}P resonance at −15.5 ppm and H_2O (Fig. 5) is slightly more intense than the one between the ^{31}P resonance at −18.4 ppm and H_2O, which is consistent with the fact that both P5 and P6 (−15.5 ppm) interact with the water

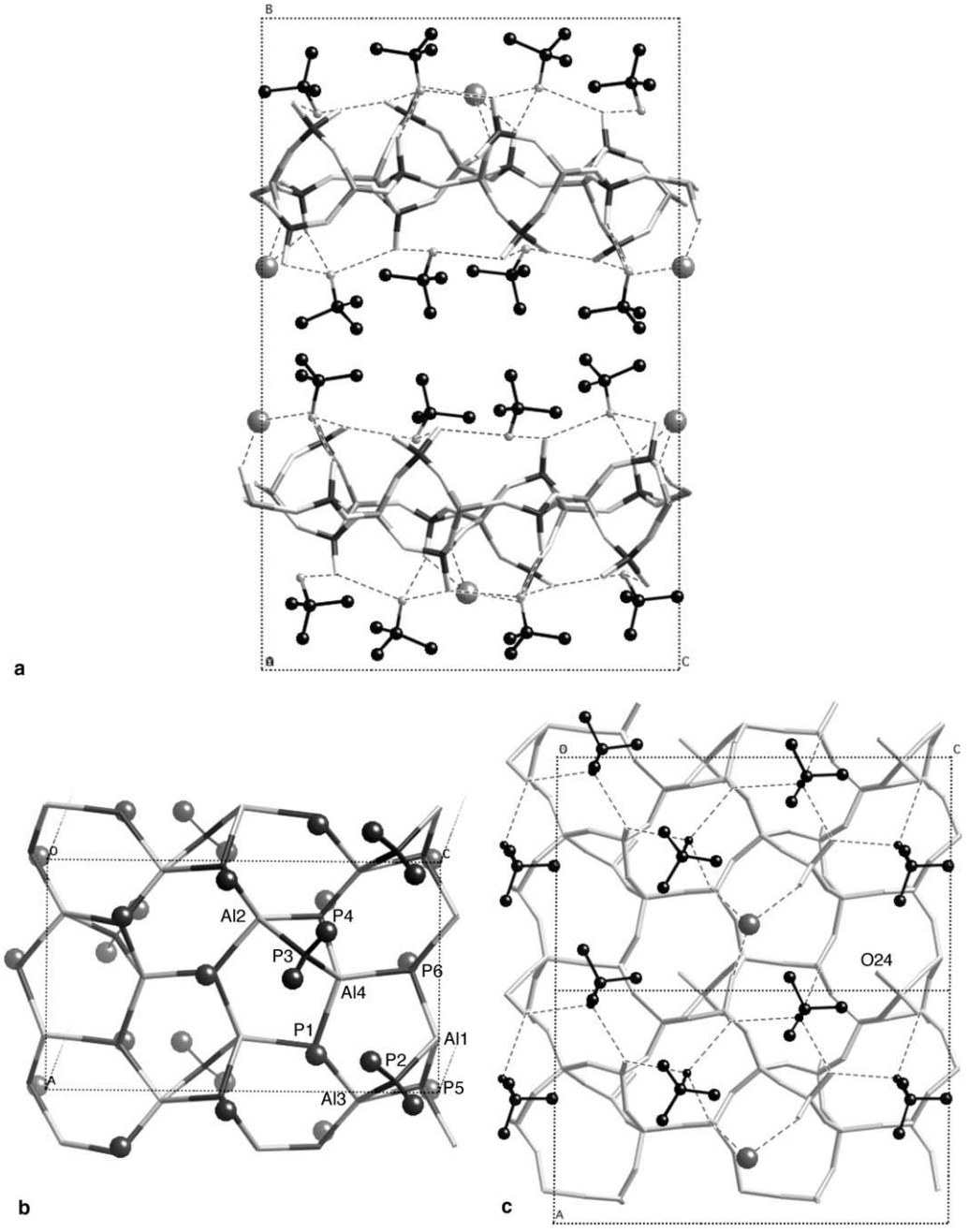

Fig. 8. Projections of the crystal structure of Mu-33. (a) Down [1 0 0] showing the full structure, and (b) down [0 1 0] showing the aluminophosphate layer, the terminal oxygens, and the Al and P numbering scheme (bridging oxygens omitted for clarity), and (c) down [0 1 0] showing the hydrogen bonding network formed by the *t*-butylammonium ions and water molecules with the terminal oxygens of the aluminophosphate layer. The terminal oxygen O24, which is not involved in H-bonding is indicated.

molecule, whereas only P3 of the −18.4 ppm resonance does.

According to the structure, P1 is connected to just one amine (via O7) whereas P4 is connected to two (via O11). Because the ^{31}P resonance at −13.4 ppm is only weakly connected to the NH_3^+ resonance of the tBA^+ cations, it must correspond to P1. Surprisingly, according to the 2D ^{1}H–^{31}P HETCOR experiment, the low field ^{31}P signal at −9.2 ppm seems to correspond to P4. The larger deshielding of this phosphorus atom could be explained by the presence of hydrogen bonds between its oxygen O11 and two amines (N6 and N11) that would pull some electron density away from the associated tetrahedron. It should be noted that the "free" water molecules observed by ^{1}H NMR (resonance at 5.1 ppm) were not detected by XRD.

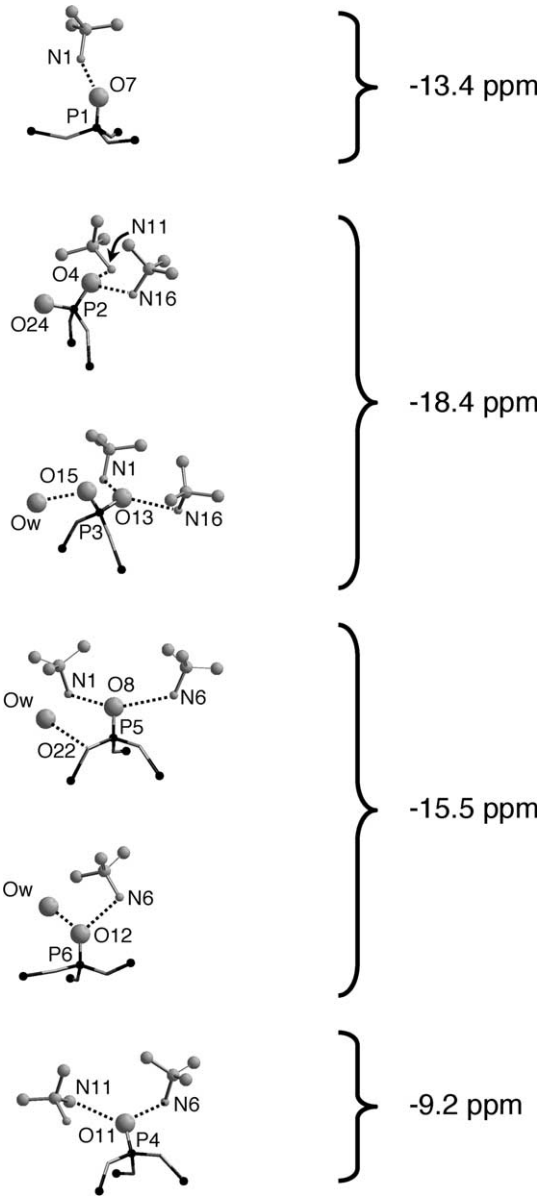

Fig. 9. Hydrogen bonding scheme (dotted lines) for each phosphorus site together with the proposed ^{31}P resonance assignment.

5. Conclusion

A new layered aluminophosphate, Mu-33, has been prepared in a quasi non-aqueous medium using *tert*-butylformamide (*t*BF) as the main solvent. As in several similar syntheses, the solvent decomposed during the synthesis, and the corresponding amine was found to be occluded in the final structure. The in situ release of the protonated amine during the synthesis appears to be a key step in the crystallization of this lamellar aluminophosphate. Indeed, experiments using *tert*-butylamine in the starting mixture directly did not lead to the crystallization of this material.

Although the structure of this new layered material could be solved from single-crystal synchrotron data collected on a microcrystal, high-resolution synchrotron powder diffraction data had to be used to obtain a satisfactory refinement. This underlines the complementarity of the two techniques. Results from X-ray diffraction and ^{13}C, ^{31}P, ^{1}H and ^{27}Al solid state NMR experiments are in very good agreement with one another. In particular, the combination of the structure analysis and the results of a ^{1}H–^{31}P HETCOR experiment allowed an assignment of each of the ^{31}P resonances to the corresponding crystallographic P site to be proposed.

Acknowledgements

It is a pleasure to acknowledge Dr. Loïc Vidal, Dr. Jean-Marc Le Meins and Dr. Michel Soulard for helpful discussions on the synthesis, XRD techniques and thermal analysis, respectively. We also thank Dr. Volker Gramlich for his assistance with the structure solution. Experimental support from the staff of the Swiss-Norwegian Beamlines at the European Synchrotron Radiation Facility in Grenoble is gratefully acknowledged. J.L.J. thanks the Spanish Secretary of State for Education and Universities and the European Social Funding for their support in the form of a postdoctoral grant.

References

[1] S.T. Wilson, B.M. Lok, C.A. Messina, T.R. Cannan, E.M. Flanigen, J. Am. Chem. Soc. 101 (1982) 1146.
[2] A.M. Chippindale, A.V. Powell, L.M. Bull, R.H. Jones, A.K. Cheetham, J.M. Thomas, R. Xu, J. Solid State Chem. 96 (1992) 199.
[3] A.M. Chippindale, S. Natarajan, J.M. Thomas, R.H. Jones, J. Solid State Chem 111 (1994) 18.
[4] A.M. Chippindale, Q. Huo, R.H. Jones, J.M. Thomas, R. Walton, R. Xu, Stud. Surf. Sci. Catal. 98 (1995) 26.
[5] S. Oliver, A. Kuperman, A. Lough, G.A. Ozin, Inorg. Chem. 35 (1996) 6373.
[6] A.M. Chippindale, A.R. Cowley, Q. Huo, R.H. Jones, A.D. Law, J.M. Thomas, R. Xu, J. Chem. Soc., Dalton Trans. (1997) 2639.
[7] Q. Gao, J. Chen, R. Xu, Y. Yue, Chem. Mater 9 (1997) 457.
[8] Q. Gao, B. Li, J. Chen, I. Williams, J. Zheng, D. Barber, J. Solid State Chem. 129 (1997) 37.
[9] L. Vidal, V. Gramlich, J. Patarin, Z. Gabelica, Eur. J. Solid State Inorg. Chem. 35 (1998) 545.
[10] S. Oliver, A. Kuperman, G.A. Ozin, Angew. Chem. Int. Ed. 37 (1998) 46.
[11] W. Tieli, Y. Long, W. Pang, J. Solid State Chem. 89 (1990) 392.
[12] K.R. Morgan, G.T. Gainsford, N.B. Milestone, J. Chem. Soc., Chem. Commun. (1997) 61.
[13] M.A. Leech, A.R. Cowley, K. Prout, A.M. Chippindale, Chem. Mater. 10 (1998) 451.
[14] L. Vidal, J.L. Paillaud, Z. Gabelica, Micropor. Mesopor. Mater. 24 (1998) 189.
[15] L. Vidal, V. Gramlich, J. Patarin, Z. Gabelica, Chem. Lett. (1999) 201.

[16] L. Lakiss, A. Simon-Masseron, V. Gramlich, J. Patarin, Solid State Sci. 7 (2005) 141.
[17] L. Lakiss, A. Simon-Masseron, J. Patarin, Microporous Mesoporous Mater. 84 (2005) 50.
[18] L. Vidal, Thesis, Université de Haute Alsace, Mulhouse, France, 1999.
[19] C. Marichal, L. Vidal, L. Delmotte, J. Patarin, Micropor. Mesopor. Mater 34 (2000) 149.
[20] P.J. Barrie, Spectroscopy of New Materials, John Wiley & Sons Ltd., 1993.
[21] CrysAlis RED, Oxford Diffraction Ltd., 2004.
[22] G.M. Sheldrick, SHELXTL, version 5.1, Bruker AXS, Inc. USA, 1997.
[23] Ch. Baerlocher, XRS-82. The X-ray Rietveld System, Institut für Kristallographie, ETH, Zürich, Switzerland, 1982.